Philosophical Magazine Letters
Vol. 89, No. 7, July 2009, 453–463

Taylor & Francis
Taylor & Francis Group

Electric polarization induced by mechanical loading of Solnhofen limestone

V. Frid[a], J. Goldbaum[bc]*, A. Rabinovitch[ce] and D. Bahat[de]

[a]*Geotechnical Department, Isotop Ltd, Canot Industry Zone, Israel;* [b]*Physics Department, Technological College, Beer Sheva, Israel;* [c]*Physics Department, Ben Gurion University of the Negev, Beer Sheva, Israel;* [d]*Geological Department, Ben Gurion University of the Negev, Beer Sheva, Israel;* [e]*Deichmann Rock Mechanics Laboratory of the Negev, Ben Gurion University of the Negev, Beer Sheva, Israel*

(*Received 21 August 2008; final version received 6 May 2009*)

Electromagnetic radiation was detected while loading a sample of Solnhofen limestone, which is not a piezoelectric material. The sample was subjected to mixed tensile and shear loading. The signals observed are associated with a fall-off in electric polarization induced by the loading, and represent the second time derivative of the polarization. The polarization is ascribed to the complicated type of loading, leading to the existence of a chosen direction, which makes polarization possible.

Keywords: electromagnetic radiation; mechanical (electric) polarization; tensile/shear loading; limestone

1. Introduction

Electromagnetic radiation (EMR) emanating during fracture has been detected in many experiments on various materials [1–9]. Propagating cracks have been shown to be a significant source of EMR, via the emission of both electrons and ions from fresh crack surfaces [10] and the collective oscillation of ions on these surfaces [6–8]. However, EMR can also be caused by a change in stress-induced electric polarization. Polarization involves the phenomena in which the centers of oppositely charged ions do not coincide [11]. As noted by Mahmudov and Kuksenko [12], polarization of solid materials under load has a lot in common with electric polarization in a weak electric field: both cause microscopic displacement of a great number of ions, which can create a significant dipole moment. Polarization caused by mechanical stress has been studied by Varotsos et al. [13] in ionic crystals, under a changing rate of both uniaxial stress and indenter penetration. These authors found that the polarization increases when the loading accelerates or decelerates.

*Corresponding author. Email: julia@bgu.ac.il

ISSN 0950–0839 print/ISSN 1362–3036 online

DOI: 10.1080/09500830903022636
http://www.informaworld.com

Similar results were observed by Ma and Cross [14] who noted that the polarization was proportional to changes (gradients) in the strain rate. The phenomenon is called flexoelectricity and appears in crystals with all symmetries.

Ogawa et al. [15] measured, by means of an electric sensor, the electric field during collision of two feldspars and also during the impact of a hammer or a falling brass sphere on a sample of granite. The detected signals comprised two parts, which were sometimes superimposed: (1) sine-like oscillations of several tens of kilohertz emitted by fracturing (which are beyond the scope of this article) and (2) a change of baseline, which was not periodic, decayed in time, and originated from a change in the material polarization. These latter signals were shown to be proportional to the depolarization current [16]. Though polarization in granite is enhanced, if not entirely caused by piezoelectricity, which is not the case for Solnhofen limestone, the similarity in shapes of the signals obtained in [15] with those given in [16–18] and in this article is evident.

In our previous EMR experiments on various materials subjected to percussion drilling [17], we detected signals of different types and classified them. Numerous sine-like signals with frequencies ranging between tens of kilohertz and several megahertz were generated during fracture (Figure 1c). However, a different type of signal was found in glass and in Solnhofen limestone, which was related to rapid material depolarization. The polarization itself was induced by unidirectional stress accumulation in the sample as a result of numerous impacts by the percussion drilling process. The depolarization process was shown to originate from the rapid stress decrease caused by fracturing. That is why crack-induced signals generally precede, or superimpose, depolarization-produced ones.

The signals we measure are of the electromotive force in an antenna-type loop, which is proportional to the second derivative of the polarization. In glass, these signals were long (10–800 μs; Figure 1a) and were preceded by another type of EMR signals [16], which are also lengthy and caused by the creation of long cracks. In Solnhofen limestone [18] the depolarization signals were much shorter (0.1–2 μs; see Figure 1b).

As is well known, the application of an electric field can lead to changes in the dimensions of solids (electrostriction effect), while no inverse effect exists. The lack of the inverse effect is due to the necessity for "symmetry breaking" for such a process. Note that while the electric field has a preferred direction, the elastic field has only a preferred axis. Therefore, under uniaxial stress, the dipoles that could have been created by displaced ions should have random orientations relative to the axis of the applied external load, which results in roughly zero polarization. How, then, can the polarization under stress lead to the results described above, and how can our own percussion drilling experiments be explained? We presume that a "strictoelectric" effect can be obtained if the necessary symmetry breaking of the movement of ions is reached in one way or another, for example, by the loading scheme. Thus, under impact, percussion drilling or indenter loading, a preferred direction defined by the velocity direction of the impinging agent is obtained and polarization becomes feasible. To check this assumption, we loaded a Solnhofen limestone sample according to a complicated procedure (see below) and examined the EMR signals obtained. Previously, we have investigated Solnhofen limestone both under uniaxial compression and during percussion drilling. In the former case,

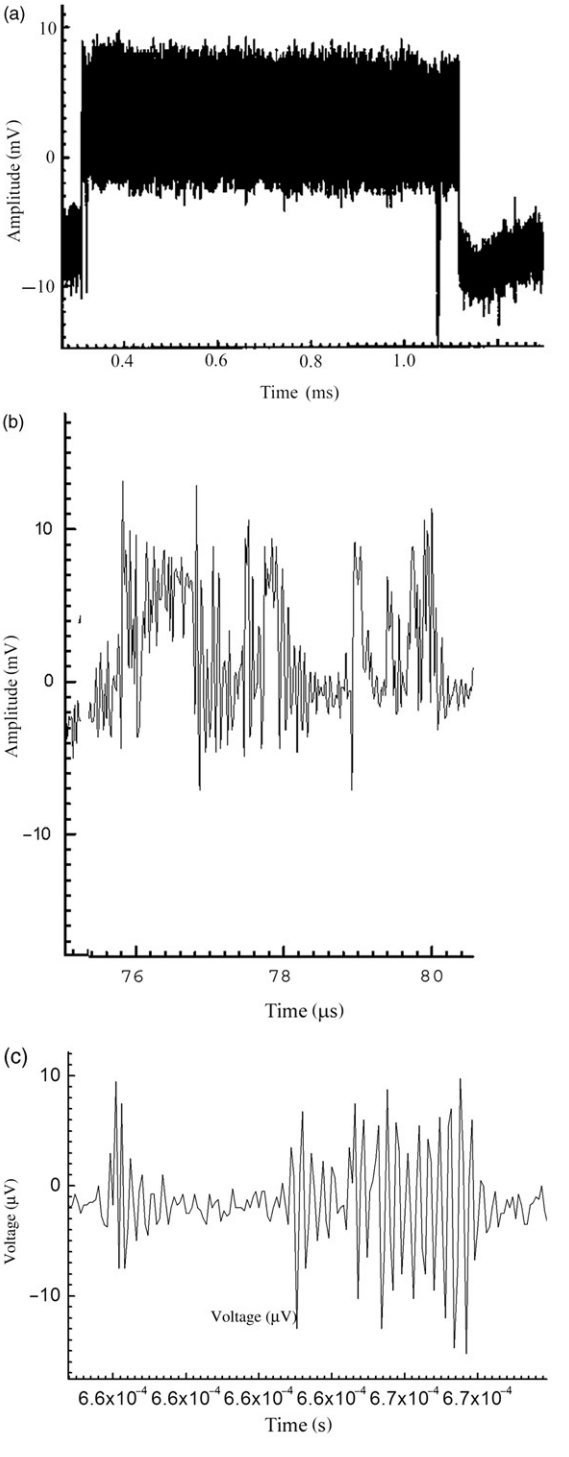

Figure 1. Polarization pulses emitted by (a) glass and (b) Solnhofen limestone samples subjected to percussion drilling (c) an example of a fracture-emitted signal.

no depolarization signals were registered, while in the latter, numerous signals associated with depolarization of the material were obtained.

2. Experimental arrangement

A TerraTek loading machine (maximal axial stress up to 100 MPa; stiffness 5×10^9 N/m) was used for the measurements. It is operated by a closed-loop servocontrol (linearity 0.05%), which is used to maintain a constant axial displacement rate of the piston. The axial load was measured with a load cell (linearity 0.5% full scale). An axial cantilever enabled us to measure strain along the sample's vertical axis.

A magnetic one-loop antenna (EHFP-30 Near Field Probe set, Electro-Metrics Penril Corporation), 3 cm in diameter, was used for the detection of the EMR. It is wound within a balanced Faraday shield, so that its response to external electric fields is vanishingly small. A low-noise micro-signal amplifier (Mitek Corporation Ltd., frequency range 10 kHz–500 MHz, gain 60 ± 0.5 dB, noise level 1.4 ± 0.1 dB throughout) and analog-to-digital converter connected to a triggered PC completed the detection equipment. The antenna was situated 2 cm away from the center of the loaded samples with its normal pointing perpendicularly to the cylinder axis.

In this study, cylindrical samples of Solnhofen limestone (10 cm long and 5.4 cm diameter) were used. The Solnhofen limestone has an average grain size of ~4 μm with serrated grain boundaries and 1–2 vol% of secondary phases (mostly clays/micas, sulfides and oxides) [19] and is not piezoelectric. Its water content is limited because of the fine-grain structure [20]. However, the samples were dried at 110°C for 24 h, because water molecules have a permanent dipole moment and may change the polarization [21].

The samples were loaded in a two-step procedure – by shear loading (Mode II) followed by a uniaxial compression. The samples were partly cut along their vertical axis in such a way that, in the middle part of each sample, an ''untouched'' area (a ''bridge'') was left (Figure 2). The depth of the pre-cut was 40 mm. Hence, two connected ''half-cylinders'' were created. The top end of one of the half-cylinders was glued by epoxy to the end-cup of the loading machine, while the bottom end of the second half-cylinder was glued to the second end-cup. The assemblage was put into the loading machine with its bottom end-cup connected to the tension machine table, while the top end-cup was connected to the moving piston. Thus, the upward displacement of the machine piston administered Mode II loading. The rate of displacement (1 μm s^{-1}) was controlled by two vertical displacement detectors and the loading machine closed servo-loop.

3. Results

Figure 3a shows the entire stress–time curve of our experiments. Negative stress corresponds to the shear mode (Mode II) of loading, while positive stress corresponds to a compressive loading. Figure 3b is a zoom-in of the graph as shown in Figure 3a. Note the two rapid oscillations beginning at times 268 and 269 s of the stress–time curve, where two EMR events were observed, are shown in Figure 3b (see arrows).

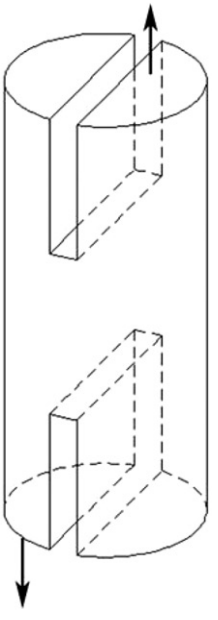

Figure 2. Solnhofen sample pre-cut along its vertical axis.

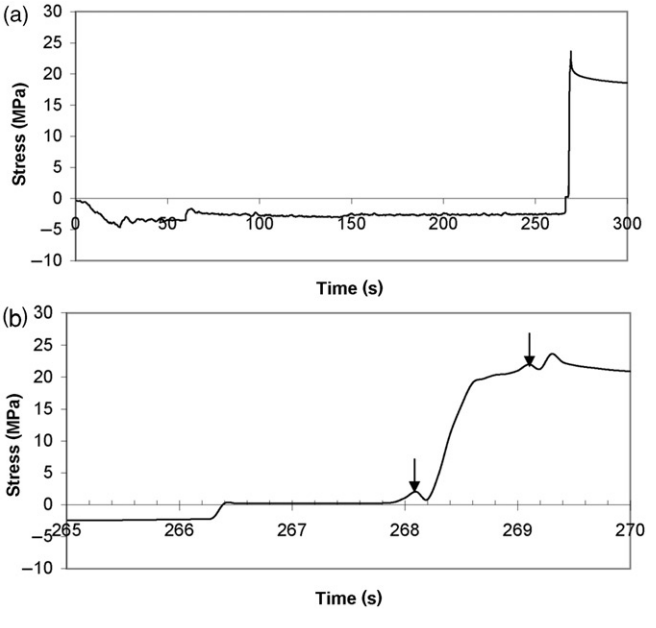

Figure 3. Stress–time curve of the Solnhofen sample subjected to two-stage deformation – (a) first, direct shear and second, uniaxial compression; (b) zoomed-in curve of sample loading – note two events of stress oscillation at 268.1 and 269.1 s after the beginning of the test, which correspond to two depolarization signals (an example of depolarization signal observed at 268.1 s is shown in Figure 4).

Figure 4a shows a part of the EMR signal that occurred at 268.1 s. It is lengthy and consists of a chain of three individual pulses (a part of which is shown in Figure 4a), whose shape is similar enough (albeit with a faster decay rate) to that observed during our percussion drilling experiment with glass (Figure 1a), indicating

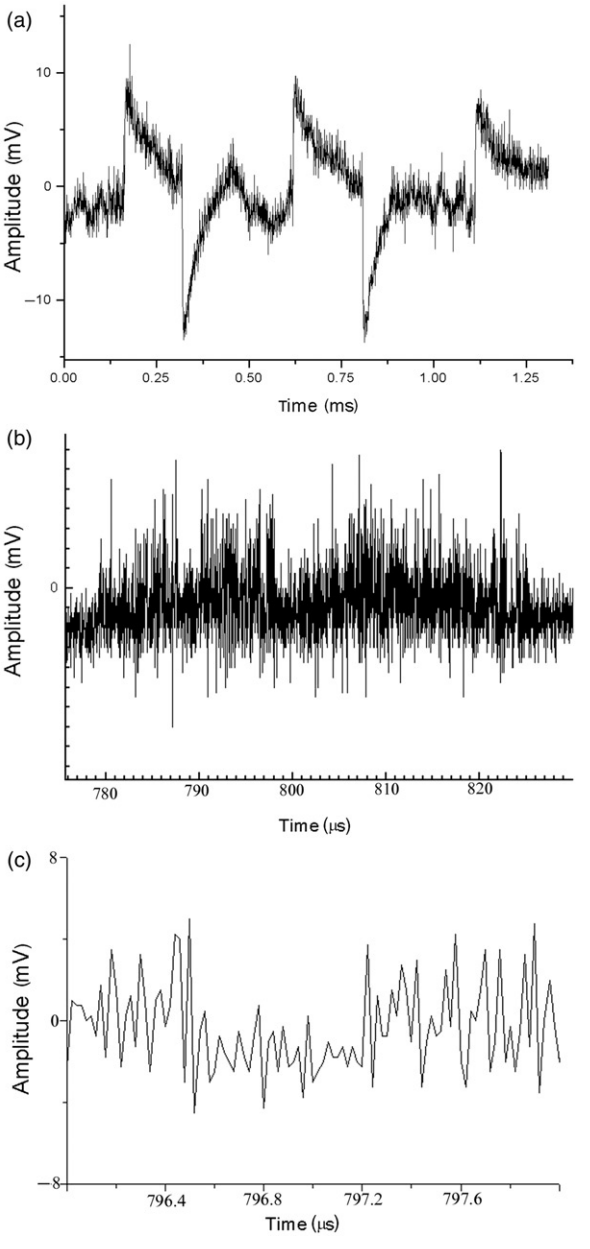

Figure 4. Depolarization signals observed in the present experiment: (a) at 268.1 s, (b) at 269.1 s, and (c) zoomed-in short section of the second signal.

a depolarization origin for the signal. Figure 4b shows a signal that consists of numerous short pulses, which are characteristic of EMR emitted from rocks and caused by depolarization. Note the similarity between Figure 4c, which is a fragment of this pulse, and Figure 1b.

4. Data processing

We are now in a position to calculate the polarization change during the signal shown in Figure 4a. The voltage in the magnetic loop antenna $A(t)$ is proportional (e.g. [16,18]) to the time derivative of depolarization current or to the polarization second derivative:

$$\ddot{p}(t) = -\frac{4\pi r^2}{S\mu_0} A(t). \tag{1}$$

Here r is the antenna-sample distance, S is the antenna loop area, and $\mu_0 = 4\pi \times 10^{-7}$ is a universal constant. Each pulse could thus represent an increase and subsequent decrease of the polarization current. Since half of each pulse is seen to decay exponentially, its shape can be expressed as

$$A(t) = \begin{cases} 0, & t < t_1 \\ A_{oi} \exp\left(-\dfrac{t - t_i}{\tau_i}\right) \quad (1 \le i \le 6), & t \ge t_1 \end{cases}. \tag{2}$$

For the first two pulses, initial times t_i, maximum amplitudes A_{0i}, and decay times τ_i are found from the graph, while for the second half of the third pulse, the amplitude can be assumed to be equal to that of its first half, and the decay time is calculated from the condition that the depolarization current is zero both at the beginning and at the end of the signal.

The polarization second derivative is thus given by

$$\ddot{p}(t) = \begin{cases} 0, & t < t_1 \\ \ddot{p}_{oi} \exp\left(-\dfrac{t - t_i}{\tau_i}\right) \quad (1 \le i \le 6), & t \ge t_1 \end{cases}. \tag{3}$$

One can now obtain by subsequent time integration (Appendix) the polarization derivative

$$\dot{p}(t) = \begin{cases} 0, & t \le t_1 \\ \dot{p}(t_i) + \ddot{p}(t_i)\tau_i \left(1 - \exp\left(-\dfrac{t - t_i}{\tau_i}\right)\right) & t_i \le t \le t_{i+1}, \end{cases} \tag{4}$$

and the polarization change

$$\Delta p = \sum_{i=1}^{6} \left\{ [\dot{p}(t_i) + \ddot{p}(t_i)\tau_i](t_{i+1} - t_i) - \ddot{p}(t_i)\tau_i^2 \left[1 - \exp\left(-\frac{t_{i+1} - t_i}{\tau_i}\right)\right] \right\}. \tag{5}$$

The numerical value of the latter is found to be $\Delta p = 5.82 \times 10^{-6}$ C m. Details are described in the Appendix section.

Let us now calculate the polarization change during the signal shown in Figure 4b. It consists of many short pulses like those shown in Figure 1b. Summing up their amplitudes and taking their average time as t_1, we estimate the polarization change using the formula [18]

$$\Delta p = -\frac{14\pi r^2}{S\mu_0} A_0 t_1^2, \tag{6}$$

where A_0 is the sum of the pulses amplitudes, r is the antenna-sample distance, S is the antenna-loop area, and $\mu_0 = 4\pi \times 10^{-7}$ is a universal constant. The value obtained is $\Delta p = 5.21 \times 10^{-8}$ C m.

5. Discussion

Polarization under stress is caused by a different response of negative and positive particles in the lattice/matrix to rapid and/or asymmetric stress application. Displacements of oppositely charged ions may be either in the opposite or in the same direction. In the latter case, polarization is obtained due to the difference in the displacements of oppositely charged particles, possibly on account of their different mobility (masses). However, if the stress is axisymmetric and stress application is gradual, individual dipoles created by the displaced ions are randomly directed in both the directions of the stress axis, and the total polarization is approximately zero. Hence, to achieve bulk polarization, at least a large part of electric dipoles must be organized in some degree of regularity. This kind of "order" can be reached only by an asymmetrical loading. It may be sample bending [12], or percussion drilling/impacts [18], or stress change fast enough to create stress nonhomogeneity (gradient) like a shock wave, which acts like an impact, or any loading with stress/strain gradient [14]. In the present experiment, the imbalance of ions displacement is achieved by applying shear loading, thus providing each "half-cylinder" with a unique direction.

Polarization mechanisms discussed in the literature include: (1) motion of dislocations, which is not appropriate for brittle materials, (2) p holes O^- in broken peroxy links [22], which cannot be activated in carbonate minerals such as calcite in limestone [23], and (3) concentration of peroxy links in glass, which is below the detection limit [22].

Recently, it has been pointed out that in percussion drilled samples of Solnhofen, polarization is accumulated by the repeated impacts [18]. A possible polarizing mechanism suggested in [18] was the displacement of the Ca^{2+} sublattice relative to the CO_3^{2-} sublattice. It is reasonable to assume that a similar relative displacement can also be reached in the case of asymmetrical displacement due to shear loading. The phenomenon described here differs from piezoelectricity. (1) Piezoelectricity takes place only in materials with particular crystallographic types and cannot occur, for example, in Solnhofen or glass. (2) Polarization caused by material piezoelectricity can take place only as a result of stress applied along a unique axis.

Using the formulas developed in [18], we can calculate the approximate relative displacement of the two sublattices that takes place during each of the two signals obtained during the test. Its minimal value is estimated by

$$\Delta l = \frac{|\Delta p|}{q},$$

where the total charge of Ca^{2+} ions is $q = 2enV$, where V is the sample volume and n the ion concentration is (taking into account the hexagonal structure) given by

$$n = \frac{2}{\sqrt{3}a^2 h}.$$

The lattice parameters are $a = 5$ Å and $h = 17$ Å [24]. Therefore, the displacement for the first signal is 0.306 Å and for the second signal is 2.72×10^{-3} Å. Both the values look reasonable, that is small relative to the lattice distance.

It is seen that the polarization change in Figure 4a is incremental, occurring in three consecutive "jumps". This behavior could be due to the uneven stress application of the apparatus.

Acknowledgements

We are thankful to Dr. H. Hertrich from Solnhofer for supplying material for our sample and to Dr. S. Palchik for useful discussions.

References

[1] A.A. Urusovskaja, Soviet Phys. Usp. 11 (1969) p.631.
[2] N.G. Khatiashvili, Phys. Solid Earth 20 (1984) p.656.
[3] J.W. Warwick, C. Stoker and T.R. Meyer, J. Geophys. Res. 87 (B4) (1982) p.2851.
[4] A. Rabinovitch, D. Bahat and V. Frid, Int. J. Fracture 71 (1995) p.R33.
[5] A. Rabinovitch, V. Frid and D. Bahat, Phil. Mag. Lett. 5 (1998) p.289.
[6] A. Rabinovitch, V. Frid and D. Bahat, Phil. Mag. Lett. 79 (1999) p.195.
[7] A. Rabinovitch, V. Frid, D. Bahat and J. Goldbaum, Isr. J. Earth Sci. 49 (2000) p.9.
[8] V. Frid, A. Rabinovitch and D. Bahat, Phil. Mag. Lett. 79 (1999) p.79.
[9] S.G. O'Keefe and D.V. Thiel, Phys. Earth Planet. Interiors 89 (1995) p.127.
[10] B.T. Brady and G.A. Rowell, Nature 321 (1986) p.488.
[11] P. Zubko, G. Catalan, A. Buckley, P.R.L. Welche and J.F. Scott, Phys. Rev. Lett. 99 (2007) p.167601.
[12] Kh.F. Mahmudov and V.S. Kuksenko, Phys. Solid State 47 (2005) p.882.
[13] P. Varotsos, N. Sarlis and M. Lazaridou, Phys. Rev. B 59 (1999) p.24.
[14] W. Ma and L.E. Cross, Appl. Phys. Lett. 86 (2005) p.072905; 88 (2006) p.232902.
[15] T. Ogawa, K. Oike and T. Miura, J. Geophys. Res. 90 (1985) p.6249.
[16] A. Rabinovitch, V. Frid, J. Goldbaum and D. Bahat, Phil. Mag. 83 (2003) p.2929.
[17] J. Goldbaum, V. Frid, A. Rabinovitch and D. Bahat, Int. J. Fracture 111 (2001) p.L15.
[18] V. Frid, J. Goldbaum, A. Rabinovitch and D. Bahat, J. Appl. Phys. 97 (2005) p.014908.
[19] J.R. Faver and R.F. Yund, Earth Planet. Sci. Lett. 161 (1998) p.189.
[20] R. Koch, Neues Jahrb Geol Palaontol Abh 245 (2007) p.103.
[21] Y. Enomoto and H. Hashimoto, Tectonophysics 211 (1992) p.337.

[22] A. Takeuchi, B.W.S. Lau and F.T. Freund, Phys. Chem. Earth 31 (2006) p.240.
[23] F.T. Freund, A. Takeuchi, B.W.S. Lau, R. Post, J. Keefner, J. Mellon and A. Al-Manaseer, Terr. Atmos. Ocean. Sci. 1 (2004) p.437.
[24] L.L.Y. Ghang, R.A. Howie and J. Zussman, *Non-silicates: Sulphates, Carbonates, Phosphates, Halides*, *Rock-Forming Minerals*, 2nd ed., Vol. 5B, Longman Group, London, 1996.

Appendix

The amplitude, beginning time, and decay time of each half pulse are taken from the fitting to Equation (2) and shown in Table A1. The second derivative of polarization for each pulse half is given by Equation (1).

$$\ddot{p}(t) = -\frac{4\pi * 0.03^2}{(\pi * 0.03^2/4) * 4\pi \times 10^{-7}} A = -12732395A.$$

It is assumed that the first derivative of the polarization, i.e. the current, is zero at the beginning and at the end of the entire signal:

$$\dot{p}(t=0) = \dot{p}(t \to \infty) = 0.$$

$\dot{p}$ is derived as a function of time as follows:

$$\dot{p}(t) = \int_{t_1}^{t} \ddot{p}(t_1) \exp\left(-\frac{t-t_1}{\tau_1}\right) \mathrm{d}t = \ddot{p}(t_1)\tau_1 \left[1 - \exp\left(-\frac{t-t_1}{\tau_1}\right)\right], \quad \text{for } t_1 \le t \le t_2.$$

For $t_2 \le t \le t_3$:

$$\dot{p}(t) = \dot{p}(t_2) + \int_{t_2}^{t} \ddot{p}(t_2) \exp\left(-\frac{t-t_2}{\tau_2}\right) \mathrm{d}t = \dot{p}(t_2) + \ddot{p}(t_2)\tau_2 \left[1 - \exp\left(-\frac{t-t_2}{\tau_2}\right)\right],$$

and so on. The polarization change during the first half of the first pulse is

$$\Delta p_1 = \int_{t_1}^{t_2} \dot{p}(t)\mathrm{d}t = \int_{t_1}^{t_2} \ddot{p}(t_1)\tau_1 \left[1 - \exp\left(-\frac{t-t_1}{\tau_1}\right)\right] \mathrm{d}t$$

$$= \ddot{p}(t_1)\tau_1(t_2 - t_1) - \ddot{p}(t_1)\tau_1^2 \left[1 - \exp\left(-\frac{t_2 - t_1}{\tau_1}\right)\right].$$

Table A1. Numerical values characteristic for the parts of the first signal.

Pulse No.	Beginning time (s)	Decay time (s)	Pulse amplitude	$\ddot{p}$ pulse amplitude ($\mathrm{C\,m\,s^{-2}}$)	$\dot{p}$ pulse amplitude ($\mathrm{C\,m\,s^{-1}}$)	Polarization falloff Δp ($\mathrm{C\,m}$)
1. Part 1	1.626×10^{-4}	6×10^{-5}	12 μV	−152.79	0	-9.04×10^{-7}
1. Part 2	3.168×10^{-4}	5×10^{-5}	−12 μV	152.79	-8.4658×10^{-3}	-6.306×10^{-7}
2. Part 1	6.188×10^{-4}	6×10^{-5}	12 μV	−152.79	-8.445×10^{-4}	-1.3379×10^{-6}
2. Part 2	8.049×10^{-4}	5×10^{-5}	−12 μV	152.79	-9.5996×10^{-3}	-9.793×10^{-7}
3. Part 1	1.11×10^{-3}	5×10^{-5}	10 μV	−127.32	-1.9772×10^{-3}	-1.4377×10^{-6}
3. Part 2	1.32×10^{-3}	6.48×10^{-5}	−10 μV	127.32	-8.2475×10^{-3}	-5.346×10^{-7}

During the second half of the same pulse it is

$$\Delta p_2 = \int_{t_2}^{t_3} \dot{p}(t)\mathrm{d}t = \int_{t_2}^{t_3} \left\{ \dot{p}(t_2) + \ddot{p}(t_2)\tau_2 \left[1 - \exp\left(-\frac{t - t_2}{\tau_2} \right) \right] \right\} \mathrm{d}t$$
$$= [\dot{p}(t_2) + \ddot{p}(t_2)\tau_2](t_3 - t_2) - \ddot{p}(t_2)\tau_2^2 \left[1 - \exp\left(-\frac{t_3 - t_2}{\tau_2} \right) \right],$$

and so on. Then these changes, whose values are given in Table A1, are summed up to yield -5.21×10^{-8} C m.